Arab J Sci Eng (2017) 42:1185–1199
DOI 10.1007/s13369-016-2374-1

RESEARCH ARTICLE - CIVIL ENGINEERING

Spatial Mapping of Groundwater Potential Using Entropy Weighted Linear Aggregate Novel Approach and GIS

Alaa M. Al-Abadi[1] · **Hamid Reza Pourghasemi**[2] · **Shamsuddin Shahid**[3] · **Hussain B. Ghalib**[1]

Received: 2 July 2016 / Accepted: 17 November 2016 / Published online: 1 December 2016
© King Fahd University of Petroleum & Minerals 2016

Abstract A novel approach for demarcation of groundwater potential by integrating entropy information theory and linear weighted aggregation method has been proposed in this study. Altun Kupri Basin in northern Iraq is selected to explain the benefits of the proposed method. Ten groundwater conditioning factors are chosen depending upon literature reviews, local conditions, and data obtainability. These layers are ground surface elevation, slope angle, plan curvature, topographic wetness index, stream power index, aquifer hydraulic head, aquifer hydraulic conductivity, depth to groundwater, total dissolved solid, and typical soil infiltration rate. Assessment of the importance of the factors in defining groundwater potential using entropy theory reveals that aquifer characteristics such as hydraulic head and hydraulic conductivity are important along with topographic factors in delineating groundwater potentiality. The hydraulic head received the highest entropy weight of 0.23, followed by hydraulic conductivity (0.17), elevation (0.14), and topographic wetness index (0.13). The other factors received entropy weights less than 0.1, which mean that they less contribute in groundwater availability in the basin. The groundwater potential index was constructed using a linear weighted aggregation of all the ten factors. Values of the groundwater potential index are classified into five classes using Jenks classification scheme: very low, low, moderate, high, and very high. Map of potential index was validated using relative operating characteristic curve. The area under relative operating characteristic is found to be 0.74, and therefore, the prediction accuracy was good.

Keywords Groundwater potential · Entropy information theory · Linear weighted aggregation · GIS · Iraq

✉ Alaa M. Al-Abadi
alaaatiaa@gmail.com

Hamid Reza Pourghasemi
hr.pourghasemi@shirazu.ac.ir

Shamsuddin Shahid
sshahid_ait@yahoo.com

[1] Department of Geology, College of Science, University of Basra, Basra, Iraq

[2] Department of Natural Resources and Environmental Engineering, College of Agriculture, Shiraz University, Shiraz, Iran

[3] Faculty of Civil Engineering, Universiti Teknologi Malaysia, 81310 Johor, Malaysia

1 Introduction

Groundwater is the major sources of water supply in many countries across the world. Globally, about 1.5 billion people depend upon groundwater for their drinking water supply and about 38% of irrigated lands are equipped for irrigation with groundwater [1]. Groundwater is considered as the main source of future water supply as it is less vulnerable and more resistant to external impacts and climatic changes [2,3]. Despite huge significance, groundwater resources are depleted in many countries and needs urgent understanding and attention [4]. The water demands are increasing as the population growth increases; therefore, it is expected the main fresh aquifers around the world will be under pressure to meet these needs [5]. Sustainable management of groundwater to preserve the reliability of this precious resource and ensure continuous supply to meet the growing water demand at the same time is a major challenge.

Knowledge on spatial and temporal distributions of groundwater resources is the most important requisite for groundwater resources management [6]. Therefore, spatial

assessment of groundwater resources is one of the most important tasks that should be considered for groundwater resources management. The traditional methods for the study of groundwater are time-consuming, expensive and sometimes unsuccessful [7]. In the last few decades, different spatial modeling techniques have been developed for assessing groundwater resources in conjunction with the great scientific advances in the areas of geographic information system (GIS) and remote sensing (RS) technologies. In particular, the abilities of GIS in data processing and storage from different sources had made the evaluation of groundwater resources easier [8].

In the last ten years, different probabilistic and artificial intelligence techniques have been integrated with RS and GIS for evaluating of groundwater potential such as frequency ratio [9,10], weights of evidence [9,11–13], artificial neural networks [11,14], evidential belief functions [15–17], and random forest [18,19]. Despite the higher capabilities of these techniques for accurate deciphering of groundwater zones and quantification of uncertainty, the main drawback is that they require data about the geographic locations of response variable (springs, flowing boreholes, borehole with specific borehole rates or more accurately well specific capacity) to train models. However, such data are often not available, especially in developing countries such as Iraq. To overcome this disadvantage, spatial delineation of groundwater potential is often deciphered using linear weighted aggregate (LWA) method in a GIS platform. The LWA involves linear integration of different thematic raster layers which are related to the possibility of groundwater occurrence to obtain the groundwater potential index (GPI). Quantify the contribution of individual factor in controlling groundwater movement and storage is a major challenge in weighted integration approach. In this context, different weighting approaches have been evolved that are mainly classified into subjective and objective. In subjective approach, weights are derived based on knowledge of expert opinion and preferential judgment of decision makers [20], while in objective approach, mathematical models are used to assign weights. To avoid subjectivity in assessing weights in GPI calculation using LWA method, this study proposed a novel approach by integrating the LWA and entropy information theory. The improved LWA was applied for delineation of groundwater potential of Altun Kupri Basin in the northern Kirkuk governorate of Iraq. The fresh aquifer of Altun Kupri Basin is widely used for different purposes such as drinking, domestic, grazing, agriculture, and industrial activities. Proper management of the groundwater resources in the basin is required for prevention of groundwater mining and deterioration of groundwater quality. The method proposed in this study will help in a rapid, but reliable assessment of groundwater potential, which in turn will help in the management of the aquifer.

2 The Study Area

The Altun Kupri Basin is located in the northeast Kirkuk Governorate of Iraq between latitudes 35°30′–35°51′N and longitude 44°04′–44°37′E (Fig. 1). The basin occupies an area of 818 km^2 having elevation ranges between 242 and 828 m above the mean sea level (Fig. 2). The basin is surrounded by two parallel mountain ranges [21]. One in the southwest of the basin is known as Kanydomlan which is considered as a part of the Baba Dome with a height of 450 m and the other in the northeast of basin is known as Kalkalan Dagh with a height of about 800 m. A small valley covered with silt and mud is permeating between these two mountain chains [22]. The elevation on the southwest side can be found to decline sharply compared to the northeast side of the basin. The middle of the basin is almost a flat land with the interference of some bends and torsions due to the presence of several simple seasonal valleys, which are filled with water through the seasonal rainfall that discharges toward the Julak valley. This constitutes the major part of natural discharge to the Little Zab River [22].

The climatic condition in the basin is characterized by hot dry summer and cold humid winter. The mean of annual total rainfall is 342.7 mm [21], and therefore, the area is categorized as semiarid. Major portion of rainfall in the area occurs during the rainy season, which lasts from October to May. Five land use/land cover classes dominate the basin, namely herbaceous rangeland (1.5%), agricultural farms (10.2%), crop land (44.8%), barren land (32%), and urban (11.2%). The distinguished physiographic units in the area are high folded, foothill zone, flat, and river terraces [23].

Geologically, the study area is a part of the foothill zone in the folded area of unstable shelf of Iraq. The unstable shelf is the strongest subsiding part of the Arabian Plate since the opening of the southern neo-Tethys in the late Jurassic [24]. The unstable shelf is thus characterized by structural trend and facies changes that are parallel to the Zagros–Taurus suture belts. Surface folds are a characteristic feature of the unit. In the study area, outcrops formations range between Miocene and Holocene [25]. The Miocene Formations are represented by Injana and Fatha Formations. Pliocene period exposed in the northeast of the basin and represented by Muqdadyi and Bai Hassan Formations along Kalkalan Dagh series, whereas the quaternary deposits (Pleistocene and Holocene) cover the center of the basin which is famously called Julak Basin. Quaternary deposits are also found on both sides of the Little Zab River represented by river terraces [23,26].

The Muqdadyi and Bai Hassan lithological units represent the main water bearing layers in the basin [23]. The aquifers mainly recharge from rainfall. The percolated rainwater moves through the gravel layer, and conglomerate of the Muqdadyi and Bai Hassan Formations. In the western

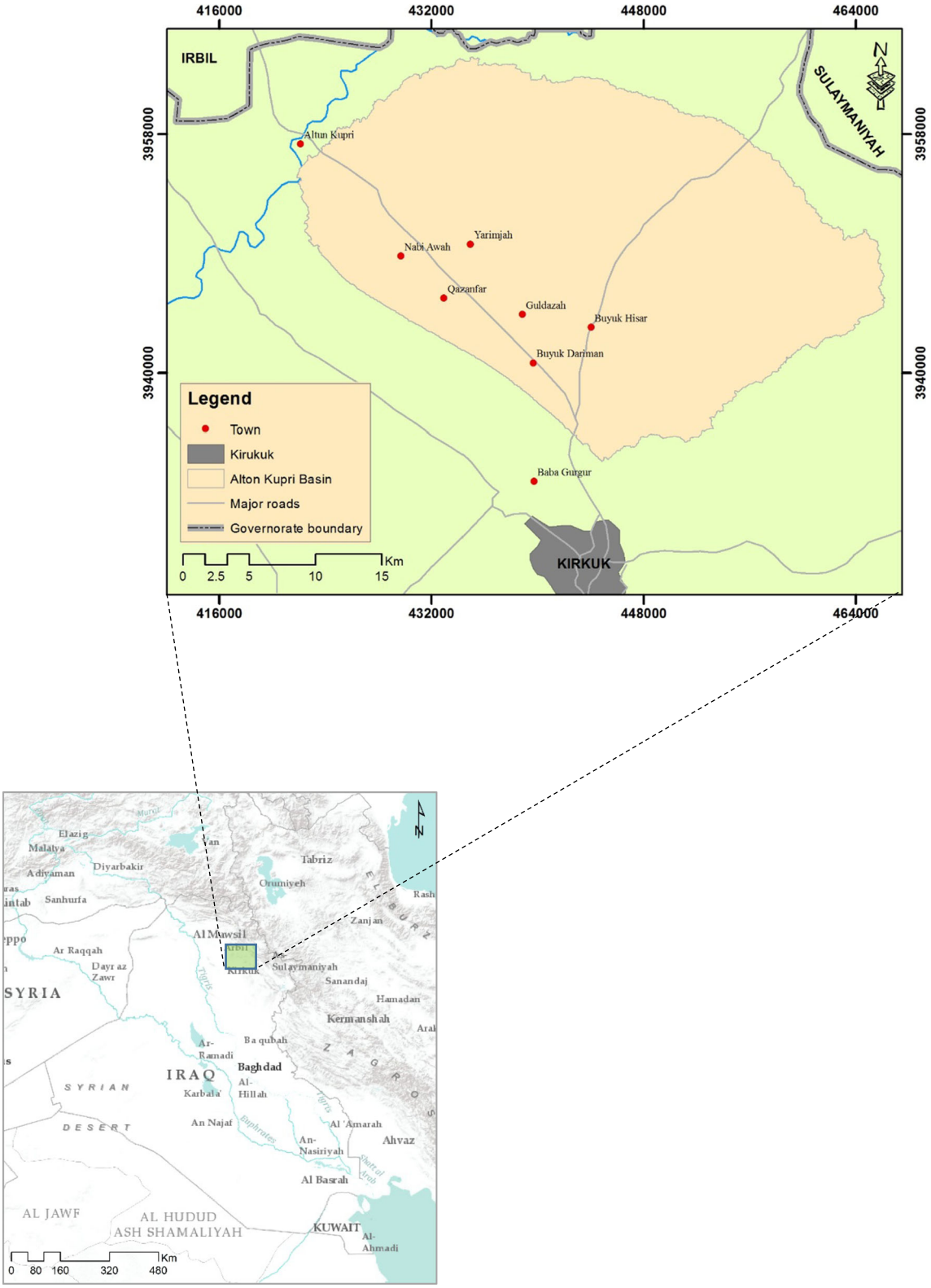

Fig. 1 Location map of the study area

part of the basin, the water flows toward northeast of the basin to Julak valley and then to the discharge area toward the Little Zab River [27]. A set of springs located in the northeast of the basin. The weathering processes on clay layers of Bai Hassan Formation lead to expose beds from sandstone or gravely sand up to clay layers, which causes

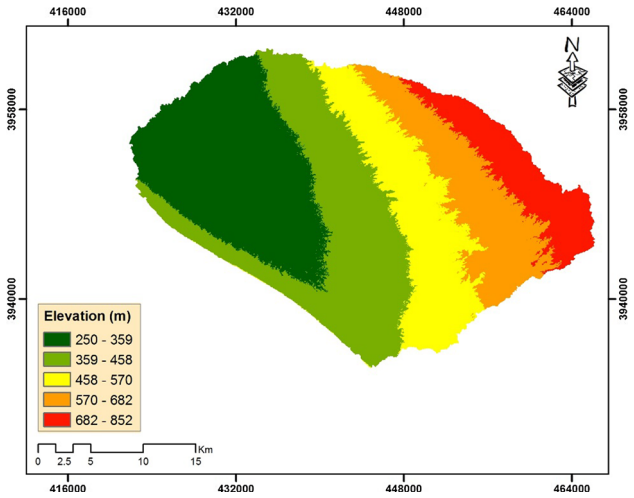

Fig. 2 Elevation (m) map of the study area

the loss of large quantities of groundwater as springs [27]. The aquifer system in the study area comprises of two water bearing units: the upper unconfined aquifer and the lower confined to semi-confined aquifers which mostly occur in Bai Hassan Formation. The thickness of the aquifer system is about 100 m in the middle of the basin, which gradually decreases to less than 50 m on the edges of the basin [28]. The average transmissivity and storativity of the upper aquifer are 3597 m^2/d and 0.053, respectively, whereas those values are 1314 m^2/d and 0.003, respectively, for lower confined or semi-confined aquifer [27]. The boundary between upper and lower aquifers is unclear; hence, the whole aquifer system is considered as a single unit for further analysis.

3 Data Used

A flowchart for clarifying the method used in this study is shown in Fig. 3. The groundwater availability of an area is controlled by different interrelated factors such as geology, structure, topography, and climate. Essentially, the aquifer system potentiality of an area could be evaluated by studying these factors and their interrelationship [28]. In this study, ten factors are used to delineate groundwater potential zones in Altun Kupri Basin. These factors are chosen depending upon literature reviews, local conditions, and data obtainability. The chosen factors are ground surface elevation above mean sea level, slope angle in degree, plan curvature, topographic wetness index (TWI), stream power index (SPI), typical soil infiltration rate, groundwater head, depths to groundwater, hydraulic conductivity, and total dissolved solid.

The catchment boundary of Altun Kupri was delineated using digital elevation models (DEM) of type (ASTER-GDEM). The ASTER-GDEM refers to Advanced Spaceborne Thermal Emission and Reflection Radiometer—Global Digital Elevation Model (ASTER-GDEM) data with a spatial accuracy of 30 m. These data are freely available from the United State Geological Survey (USGS) platform (*earthexplorer.usgs.gov*). Four tiles of ASTER-GDEM were downloaded, merged to new mosaic raster, and reprojected to Universal Transverse Mercator (UTM) projected coordinate system with WGS 1984, 38N Datum. The ArcHydro Extension tool in ArcGIS 10.3 is used to delineate basin through sequential steps beginning with fill voids in DEM, calculation of flow direction, flow accumulation, stream definition, stream segmentation, catchment grid delineation, catchment polygon processing, drainage line processing, adjoining catchment processing, and finally select an outlet point to run the batch watershed delineation. Output obtained in different steps of the catchment delineation process is shown in Fig. 4a–h. The slope degree, plan curvature, TWI, and SPI are created using DEM. The importance of these factors for delineating groundwater potential is explained in detail in previous studies [9,29–33]. For classifying continuous values, manual and Jenks classification schemes are used through this study. The Jenks classification scheme is a data clustering method designed to place variable values into naturally occurring data categories [13]. The Jenks method minimizes the variance within classes and maximize variance between classes [34].

Elevation map of the study area (Fig. 2) is directly derived by classifying the filled and reprojected DEM into five classes: 250–359, 359–458, 458–570, 570–682, and 682–853 m. The raster map of slope degree (Fig. 5a) is also directly produced by classifying the DEM into four classes: <5°, 5–15°, 15–30°, and 30–50°. Curvature raster layer (Fig. 5b) is produced from DEM and manually classified into three categories, namely concave, flat, and convex. The TWI and SPI are calculated using the following equations [35]:

$$TWI = \ln\left(\frac{a}{\tan\beta}\right) \quad (1)$$

$$SPI = A_s \tan\beta \quad (2)$$

where a is the cumulative unslope area draining through a point, tan β is the local slope in degrees at the point, and A_s is the specific catchment area. Both factors are computed using the Raster Calculator in ArcGIS 10.3 and classified into five classes (Fig. 5c, d).

The groundwater head, depth to groundwater, aquifer hydraulic conductivity, and total dissolved solid data are acquired from the archive of drillings boreholes in the basin, which is available from General Commission of Groundwater, Ministry of Water Resources of Iraq. The available data at 25 boreholes for these conditioning factors are presented in Table 1. All the 25 boreholes except three (W12, W21, W23) are within the boundary of Altun Kupri Basin. The thematic maps of groundwater controlling factors are pre-

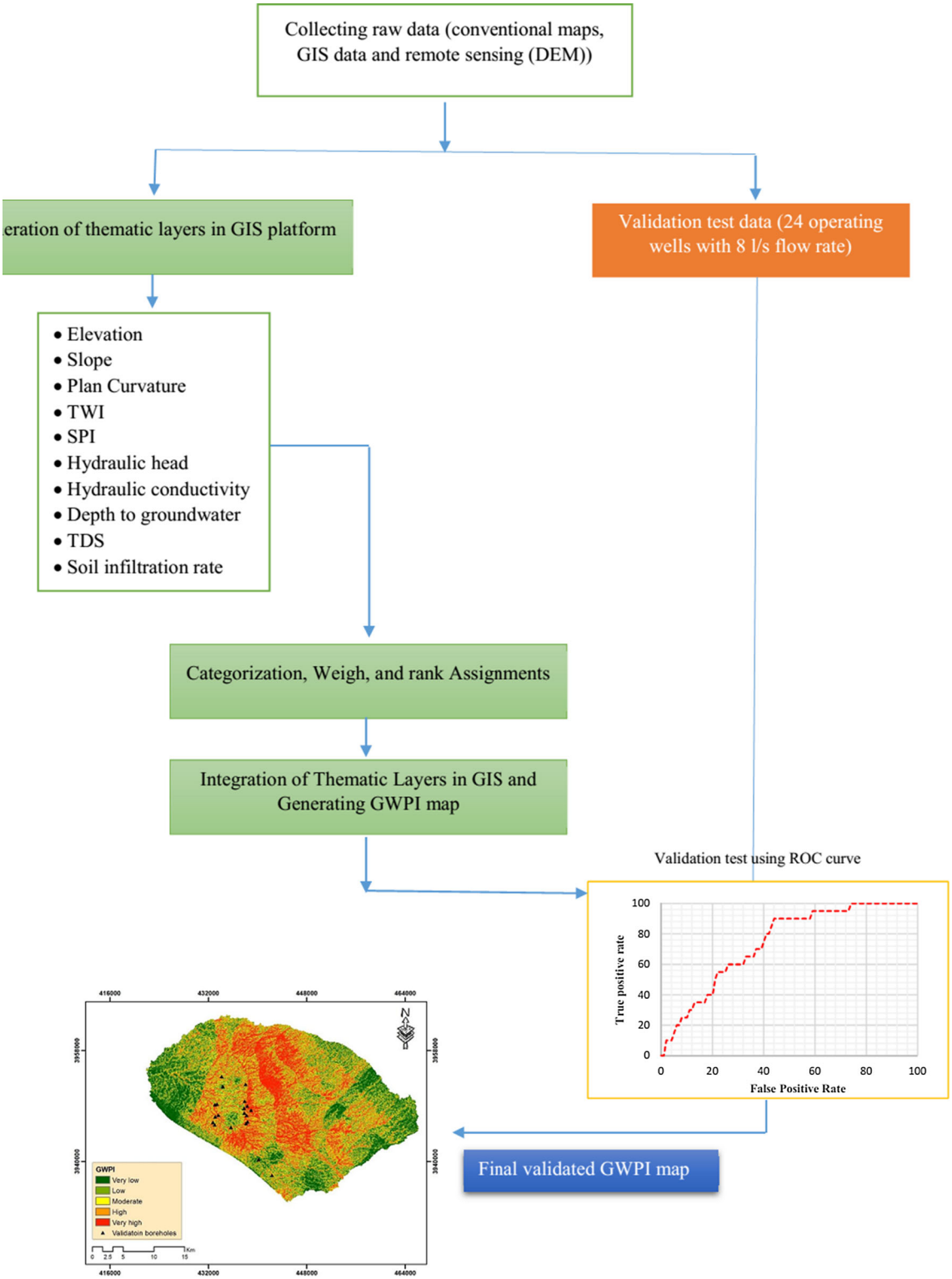

Fig. 3 Flowchart for delineating groundwater potential in Altun Kupri Basin using proposed method

pared using ordinary Kriging interpolation method. Kriging is a group of geostatistical techniques used to interpolate the value of a random filed in an unobserved location from observation of neighboring values [36]. Kriging is built on the assumption that things that are close to each other are more similar than those farther away. The detail description

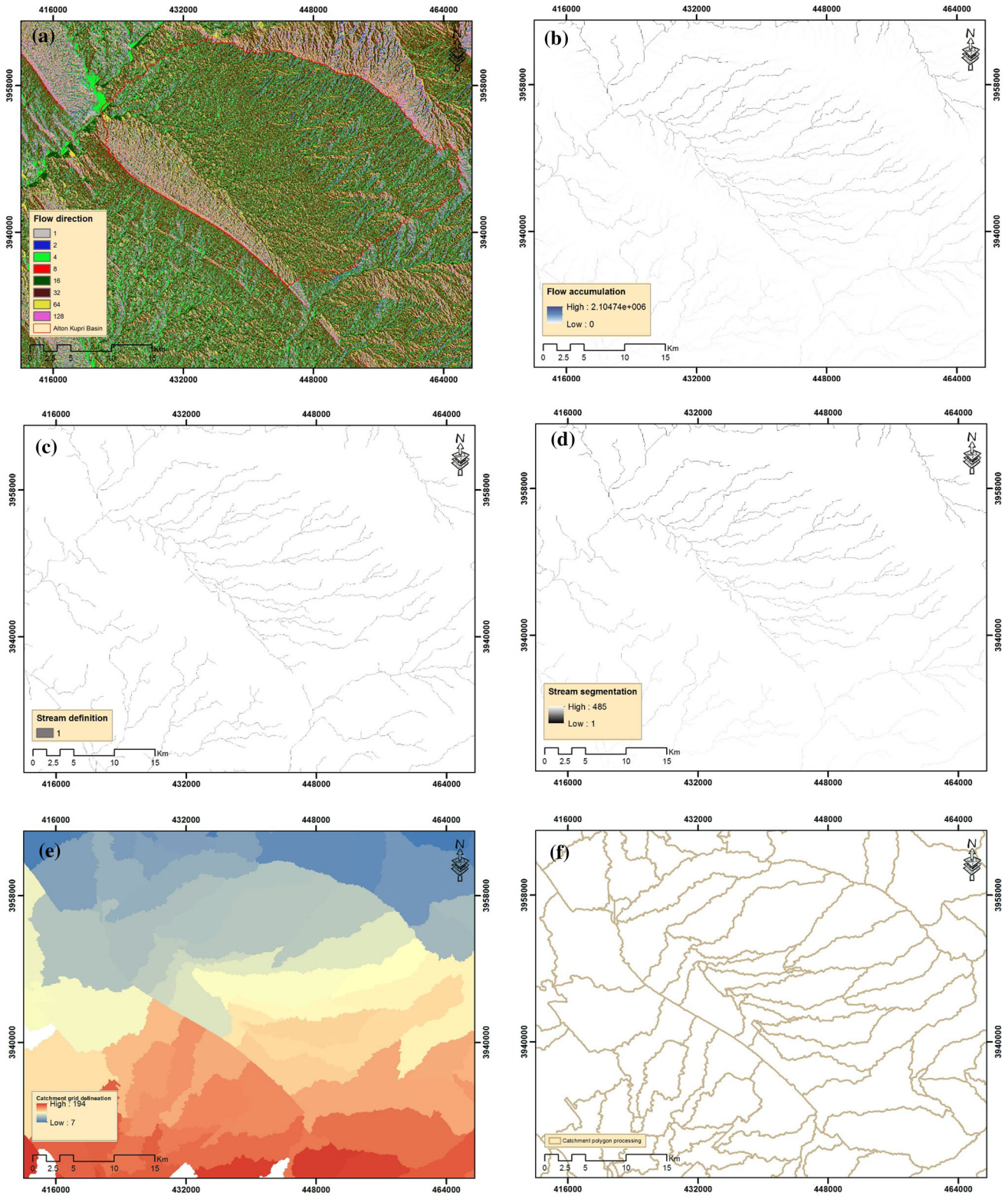

Fig. 4 Steps for delineation Altun Kupri Basin using DEM and ArcHydro tool in ArcGIS environment **a** flow direction, **b** flow accumulation, **c** stream definition, **d** stream segmentation, **e** catchment grid delineation, **f** catchment polygon processing, **g** drainage line processing, **h** Basin delineation

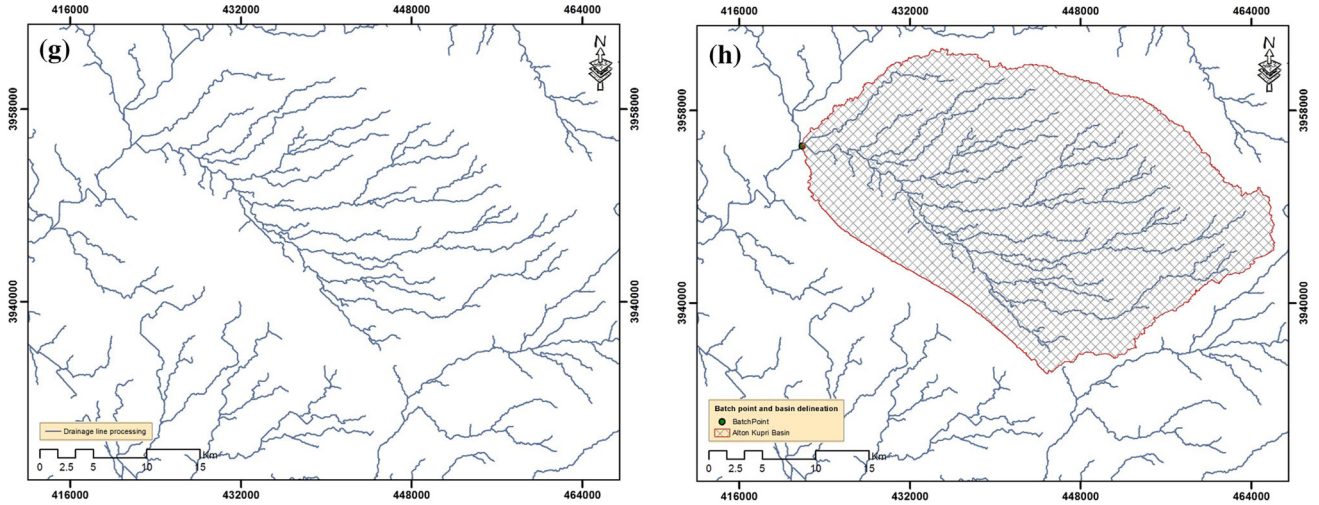

Fig. 4 continued

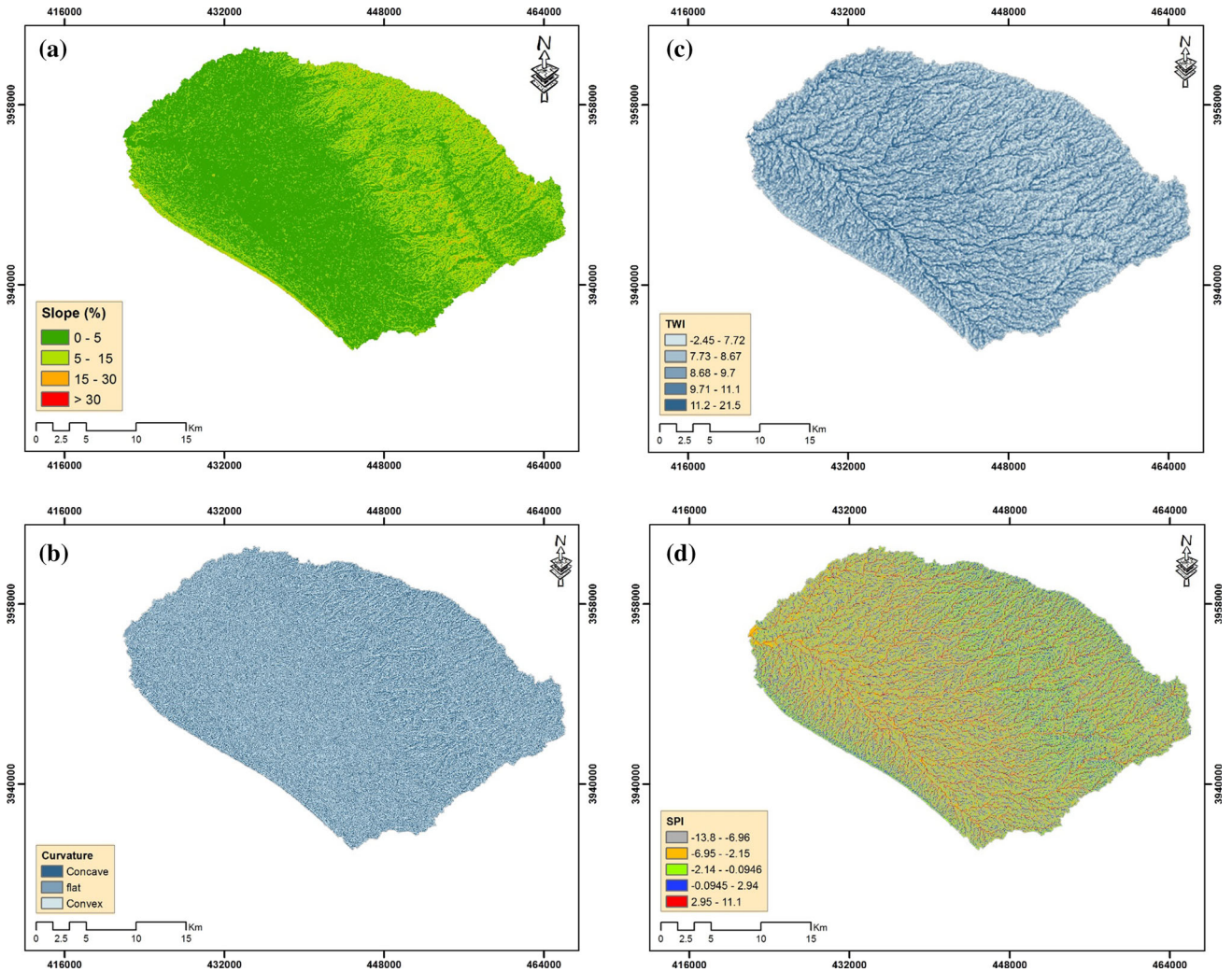

Fig. 5 Groundwater factors: **a** slope angle (%), **b** plan curvature, **c** TWI, **d** SPI

Table 1 Available data of Altun Kupri main aquifer

Geographic location (UTM)		Borehole name	Depth to groundwater level (m)	Hydraulic head (m)	Hydraulic conductivity (m/d)
Easting	Northing				
442815	3936963	w1	14	394	7.31
443219	3941089	w2	31.08	374	14.14
441940	3953298	w3	13.56	400	–
436612	3953088	w4	47	304	19.65
439317	3940838	w5	24.3	350	11.38
436742	3943197	w6	24.7	340	62
431236	3946750	w7	40	297	97.22
424462	3951489	w8	72	253	62
425314	3957151	w9	50	249	–
446934	3943870	w10	23	408	19.92
448724	3935911	w11	66	429	10.34
453022	3934655	w12	10	452	–
453267	3942941	w13	8.5	467	–
445277	3948471	w14	24	410	15.49
442713	3952430	w15	26	405	–
440817	3950748	w16	56	338	105.79
435812	3946716	w17	20	315	6.26
434243	3952089	w18	18.2	300	11.16
436351	3951704	w19	25.08	310	30.13
431197	3957904	w20	–	–	171.0
440357	3964462	w21	17.5	306.5	–
428042	3959100	w22	40	252	–
425929	3961552	w23	–	276	–
449236	3955040	w24	72	514	–
445588	3958297	w25	37.3	530.7	

of Kriging technique and its applications can be found in [37]. In general, three main steps are required to build Ordinary Kriging (OK) model: (1) Construction of a variogram from available points data. The variogram determine the spatial continuity of a data set. Variogram analysis consists of the experimental variogram and the variogram model fitted to the data. (2) Fitting a model to variogram graph. This is done by defining a line that provides the best fit through the points in the experimental variogram cloud graph [38]. (3) Computation of the weights of the Kriging equations for prediction. The best estimator is calculated mathematically as [39]:

$$\hat{Z}(x_\circ) - \mu = \sum_{i=1}^{n} \lambda_i \left[Z(x_i) - \mu(x_\circ) \right] \tag{3}$$

where μ is a known stationary mean, λ_i is Kriging weight, n is the total number of available point to be interpolated, and $\mu(x_\circ)$ is the mean of data point within the search window. Before interpolation of each groundwater factor using the best technique, comprehensive data exploratory analyses are done. These analyses involve testing of normality and trend analysis. The interpolated surfaces are classified into five categories using Jenks classification method to prepare the thematic maps of these factors. The thematic maps of groundwater head, aquifer saturated thickness, depth to groundwater, and TDS are shown in Fig. 6a–d.

Figure 6a shows that the groundwater head decreases from southeast to northwest following the elevation of the study area. The minimum, maximum, and average heads in the study are found at 249, 531, and 383 m, respectively. The lowest head is observed in flat areas close to the outlet of the basin into Zab River, while maximum values are noticed at elevated areas. The groundwater depth map is shown in Fig. 6b. The observed minimum, maximum, and average depths to groundwater level are found 9, 70, and 33 m, respectively. The highest depth to groundwater level is observed in the north and northwest parts of the study area, while the lowest depth is found in the east and central parts. Map of the hydraulic conductivity reveals that the lowest hydraulic conductivity increases from southeast toward northeast. The minimum,

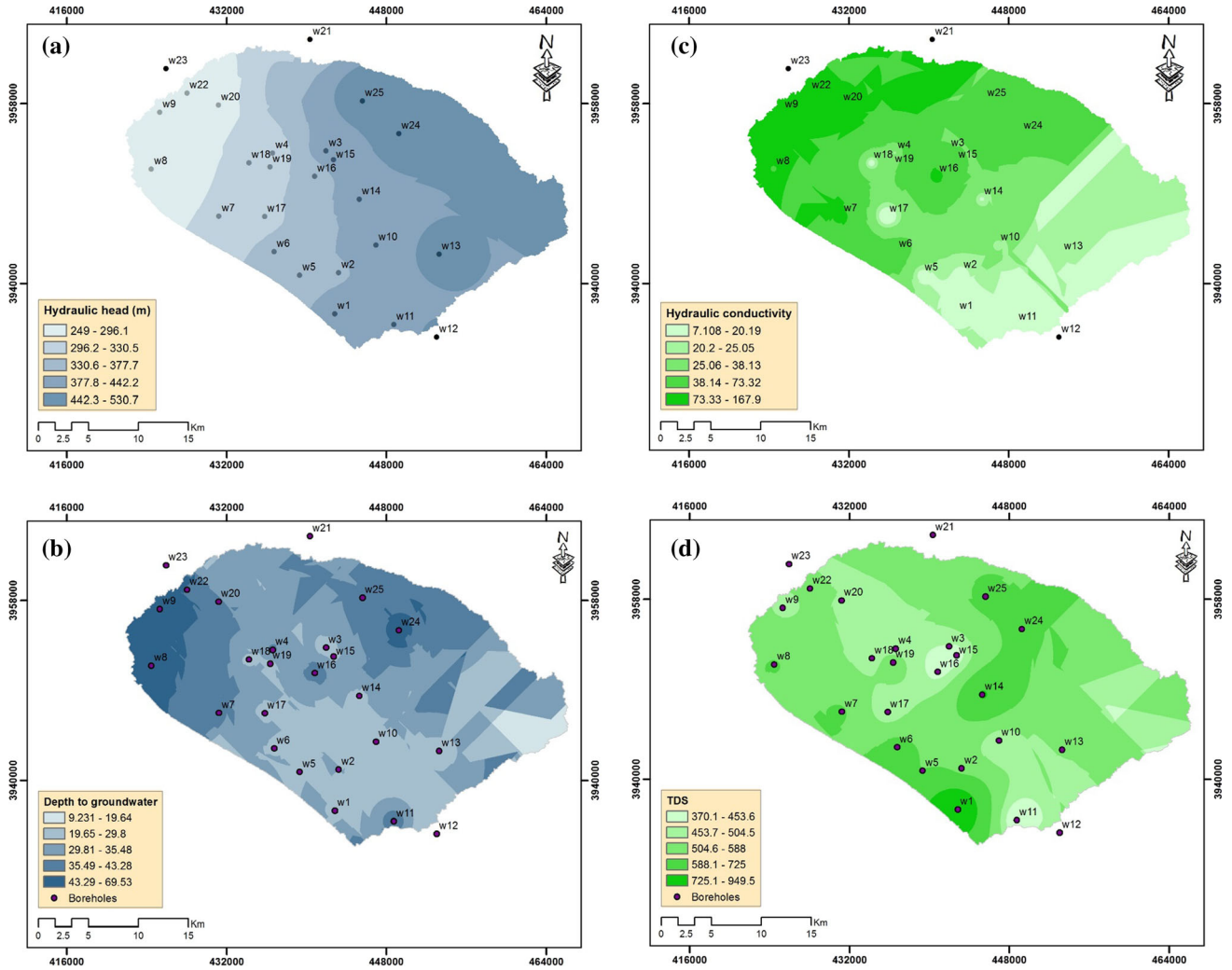

Fig. 6 Groundwater factors **a** hydraulic head, **b** depth to groundwater (m), **c** hydraulic conductivity (m/d), **d** TDS (mg/l)

maximum, and average values of hydraulic conductivity are 7.10, 168, and 43.2 m/d, respectively. The quality of groundwater is as much important as the quantity. However, most of the previous studies ignored the quality of groundwater in potential analysis and focused only on the quantity and its spatial zonation. In the present study, total dissolved solid (TDS) is considered as a factor for groundwater potential mapping. TDS is a measure of the total amount of minerals dissolved in water and therefore widely used for evaluation of water quality [40]. The results of chemical analysis of groundwater samples during the dry period when chemical concentrations are at the highest level is given in Table 2. TDS values from Table 1 are interpolated to produce the raster layer of TDS over the study area as shown in Fig. 6d. The minimum, maximum, and average values of TDS in the study area are 370, 950, and 544 gm/l, respectively. According to the World Health Organization standards for suitability of water for drinking purposes [41], groundwater of Altun Kupri Basin is fresh and could be used for drinking (Table 2) as the TDS values are less than 1000 mg/l.

To create a hydrological soil group (HSG) map of the study area, 22 soil samples were collected from different sites having different geological units. The soil samples were assigned texture types using online soil texture triangle (http://soil.usda.gov/technical/aids/investigations/texture/) based on the results obtained using sieve and hydrometer analyses in the Engineering Lab of Geology Department, Basra University, Iraq. The hydrological soil properties and their compositions are defined by the United State Department of Agriculture (USDA) with other relevant factors depending on the twelve soil textures. Following the USDA hydrological soil group classification method, samples of the study area are assigned HSG as shown in Table 3. The areal distribution of soil groups is shown in Fig. (7).

Table 2 Chemical analysis of groundwater samples (dry period)

Boreholes name	K^+	Ca^{2+}	Mg^{2+}	Na^+	SO_4^-	Cl^-	HCO_3^-	NO_3^-	TDS	T	pH
	mg/l									°C	–
W1	1.5	186	24	43	382	60	212	34	950	28.8	7.9
W2	0.8	119	11	17	210	20	160	20.5	550	25.9	8.0
W3	0.6	100	10	7	101	35	184	18.5	450	25	8.0
W4	0.8	97	12.4	10	120	15	207	27.7	468	25.2	8.0
W5	2.4	108	10	46	148	70	195	21.2	588	24.3	8.0
W6	0.8	138	18	10	190	33	238	27.9	633	24.2	7.8
W7	0.9	122	17	12.8	198	21	204	26	600	25.9	8.2
W8	0.8	112	24	18.3	167	40	230	24	596	26.2	7.9
W9	1.2	100	11	17.8	145	23	182	23.7	488	26	8.0
W10	0.8	77	16	13	80	28	199	13.6	450	25.4	8.4
W11	0.4	64	14.5	16.6	71	30	168	22	370	28.4	8.1
W13	0.4	95	22	10	149	27	190	19	510	27.3	8.1
W14	1.6	140	22	43.8	277	66	188	15	750	28	7.9
W15	1.6	75	19.4	6.6	123	10	170	14.5	410	26	8.0
W16	0.8	71	22	13	132	18	162	20	422	26.3	8.0
W17	0.7	82	19	14	142	19	169	22	451	25	7.9
W18	0.9	92	15	13	147	14	180	20.5	473	26.9	8.0
W19	0.6	120	13	16	190	33	171	19	549	25.2	7.9
W20	0.9	99	17	13.8	198	14	147	24	500	25.6	8.0
W22	0.7	120	9	13	216	18	138	28	518	24.9	8.0
W24	1.8	120	8	52	219	85	120	12.5	613	28.1	8.0
W25	1.5	120	7	60	240	88	102	13	622	27.2	8.2

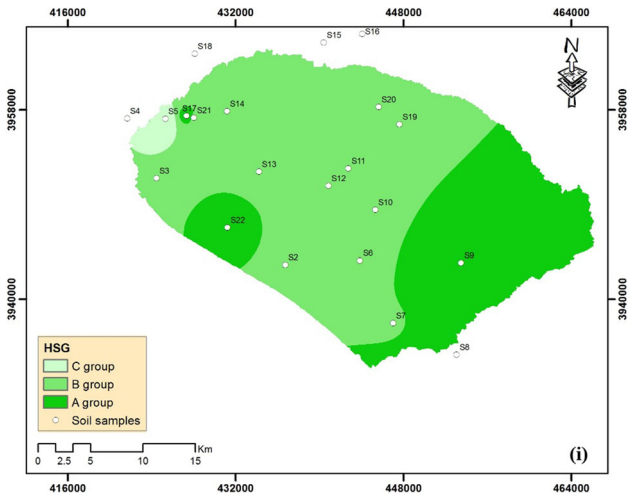

Fig. 7 Groundwater factors HGS

4 Modeling Techniques

4.1 Linear Weighted Aggregate (LWA) Method

LWA is a weighted average-based technique in which the continuous criteria are normalized to a common numeric scale and combined using a weighted average [42]. The assigned weights either subjectively or objectively are used along with standardized criteria as input for the LWA. The total score is obtained as a sum of the product of each criteria and its weight as follows [43]:

$$GWPI = \sum_{i=1}^{n} w_i x_i \tag{4}$$

where $GWPI$ is groundwater potential index; w_i is the weight of factor i, and x_i is the criterion score or rating of factor i.

4.2 Entropy-Based Weighting Approach

The entropy indicates the extent of the instability, disorder, imbalance, and uncertainty of a system [44]. Information entropy is the measurement of the disorder degree of a system. It can measure the amount of useful information with provided data. The entropy is small when the difference of the values among the evaluating objects on a parameter is high, which illustrates that the parameter provides more information, and therefore, the weight of the parameter should be set high [45]. If the difference of the values among the evaluating objects on a parameter is smaller, the entropy is higher

Table 3 Soil characteristics of the study area

Sample no.	Easting	Northing	Gravel (%)	Sand (%)	Silt (%)	Clay (%)	Soil texture	HSG
S1	442815	393696	2	67	17	14	Sandy loam	B
S2	436742	3943197	5	55	27	13	Sandy loam	B
S3	424462	3951489	20	26	31	23	Loam	B
S4	421648	3957213	29	36	25	10	Sandy loam	B
S5	425314	3957151	11	47	21	21	Sandy clay loam	C
S6	443813	3943612	6	65	18	11	Sandy loam	B
S7	446972	3937708	18	46	18	18	Sandy loam	B
S8	453022	3934686	14	69	11	6	Loamy sand	A
S9	453470	3943402	26	58	8	8	Loamy sand	A
S10	445277	3948471	6	37	30	27	Loam	B
S11	442713	3952430	10	54	20	16	Sandy loam	B
S12	440817	3950748	10	62	17	11	Sandy loam	B
S13	434243	3952089	4	53	24	19	Sandy loam	B
S14	431197	3957904	4	68	19	9	Sandy loam	B
S15	440357	3964462	6	64	20	10	Sandy loam	B
S16	444025	3965270	1	29	48	22	Loam	B
S17	427326	3957442	7	79	9	5	Loamy sand	A
S18	428102	3963382	20	58	9	13	Sandy loam	B
S19	447587	3956621	8	50	22	20	Sandy loam	B
S20	445588	3958297	14	56	16	14	Sandy loam	B
S21	428027	3957251	6	57	25	12	Sandy loam	B
S22	431236	3946750	12	77	7	4	Loamy sand	A

and the relative weight would be smaller [46]. Therefore, the information entropy theory gives weights with an objective way.

The steps used for calculation of weights using entropy method are described here. If m factors are taken to evaluate the groundwater potentiality of an area, and n randomly representative values are taken ($j = 1, 2, \ldots, n$) for each factor, then the eigenvalue matrix X can be constructed from real data as [47]:

$$X = \begin{bmatrix} x_{11} & x_{21} & . & x_{1n} \\ x_{21} & x_{22} & . & x_{2n} \\ . & . & . & . \\ x_{m1} & x_{m2} & . & x_{mn} \end{bmatrix} \tag{5}$$

To make the data dimensionless, a standardization process is implemented. In this study, the standardization Eqs. (6) and (7) were used [48,49]:

For the cost type or larger the better:

$$y_i = \frac{x_i - x_{i(\min)}}{x_{i(\max)} - x_{i(\min)}} \tag{6}$$

For the efficiency type or smaller the better:

$$y_i = \frac{x_{i(\max)} - x_i}{x_{i(\max)} - x_{i(\min)}} \tag{7}$$

where i is the index, x_i is the original value of i, $x_{i(\max)}$ and $x_{i(\min)}$ are the maximum and minimum values of original data. Equations (6) and (7) standardize the original data into a range between 0 and 1. The standardization process yields the standard-grade matrix Y as:

$$Y = \begin{bmatrix} y_{11} & y_{21} & . & y_{1n} \\ y_{21} & y_{22} & . & y_{2n} \\ . & . & . & . \\ y_{m1} & y_{m2} & . & y_{mn} \end{bmatrix} \tag{8}$$

The ratio of index value of the j index in i instant is calculated as:

$$P_{ij} = \frac{y_{ij}}{\sum_{i=1}^{m} y_{ij}} \tag{9}$$

The information entropy is computed by the following equation [48]:

$$e_j = -\frac{1}{\ln m} \sum_{i=1}^{m} P_{ij} \ln P_{ij} \tag{10}$$

The smaller the value of e_j, the bigger the effect of j index. The entropy weight is computed using Eq. 8:

$$w_j = \frac{1 - e_j}{\sum_{j=1}^{n} (1 - e_j)} \tag{11}$$

To assign ratings needed for applying WLA (Eq. 4), analytical hierarchy process (AHP) method is used. The AHP is a multi-criteria decision-making method that allows the user to get a scale of preferences drawn from a set of alternatives [49]. The AHP method takes a pairwise comparison as an input using a point scale to represent individual judgments when comparing each pair of factors [50]. It creates a ratio matrix through creating relative weights as outputs. In order to measure the consistency of subjective judgment, Satty [50] proposed what is called consistency ratio (CR) which is a comparison between consistency index (CI) and random consistency index (RI). CR is calculated as:

$$\mathrm{CR} = \frac{\mathrm{CI}}{\mathrm{RI}} \tag{12}$$

If CR is smaller or equal to 10%, the judgments are consistent to be acceptable. A *CR* equal to 0 means that judgment is totally consistent [51]. The *CI* can be computed as:

$$\mathrm{CI} = \frac{\lambda_{\max} - n}{n - 1} \tag{13}$$

where $\lambda_{\max}$ is the largest eigenvalue of comparison matrix and n is the order of the comparison square matrix.

5 Applying the Concepts

All factors used in this study for spatial zoning of groundwater productivity are prepared as raster maps in ArcGIS 10.2 with 30 m spatial accuracy. The obtained rasters are converted to ASCII format and organized in column vectors. The entropy weights are calculated from these vectors using Eqs. (5)–(11) in Microsoft Excel 2013. The formula 'smaller the better' (Eq. 7) is used for standardization of elevation, slope, plan curvature, SPI, depth to groundwater level, and TDS. The 'larger the better' normalization formula (Eq. 6) is applied for other remaining factors. Weights obtained using Eqs. (8)–(11) are summarized in Table 4. Entropy weights are also used as an indicator for importing of a factor in defining groundwater potentiality. The highest entropy weights are obtained for the hydraulic head (0.233), hydraulic conductivity (0.136), elevation (0.172), and TWI (0.136). The entropy weights for other factors are found to be less than 0.1, which indicate that they play a secondary role in groundwater occurrence. The present study confirmed the fact of higher influence of aquifer characteristic along with topographic factors in defining groundwater potential.

The groundwater potential of Altun Kupri Basin is produced using all the factors through applying (Eq. 4) using

Table 4 Calculated entropy weights for delineating GWPI in the Altun Kupri Basin

Factors	Weight
Elevation	0.1720
Slope	0.0257
Curvature	0.0554
TWI	0.1341
SPI	0.0859
Depth to groundwater	0.0666
Hydraulic head	0.2333
Hydraulic conductivity	0.1359
TDS	0.0244
HSG	0.0668
Sum	1.000

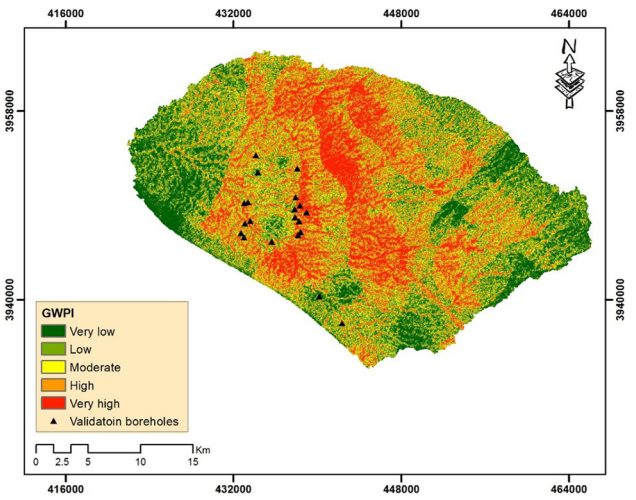

Fig. 8 GWPI map of the study area

Raster Calculator. The resultant GWPI values are found in the range of 2.16 to 4.21. The GWPI values are classified into five classes (Fig. 8): very low (2.16–2.96), low (2.96–3.12), moderate (3.12–3.27), high (3.27–3.43), and very high (3.47–4.20). Very low to low groundwater potential zone is found to cover an area of 327 km^2. The moderate groundwater potential zone is found to cover an area of 164 km^2. On the other hand, aquifer in about 327 km^2 is found to have high and very high potential. With respect to spatial zoning of groundwater availability, the high groundwater potential zones are found in the central and northern parts of the basin, where the hydraulic head and hydraulic conductivity are moderate to high. Areas with gentle flat slope, moderate soil infiltration rate, smaller TDS, and smaller depth to groundwater fall under moderate to high groundwater potentiality. The western and southwestern parts of the basin have very low to low potential zones. The moderate potential zone is distributed sparsely through the study area.

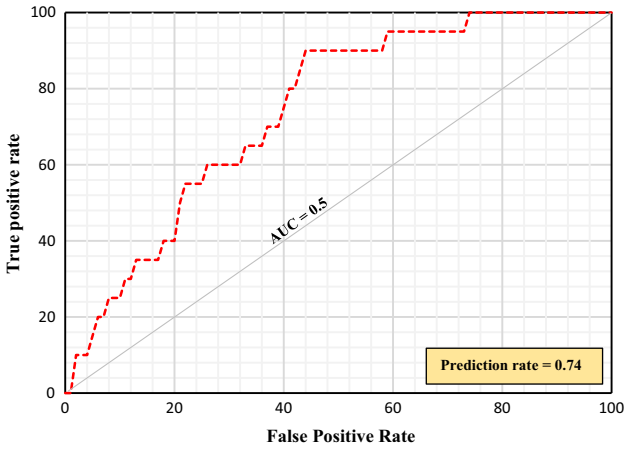

Fig. 9 ROC curve

To validate GWPI map, the relative operating characteristic (ROC) curve was used. The ROC curve is a graphical plot essentially used in the binary classification to examine the output of a classifier. This plot is typically generated by plotting the 1- specificity (false positive rate) on *X*-axis versus the sensitivity (sensitivity (true positive rate) on the *Y*-axis at different threshold settings [51]. The area under the ROC curve (AUC) characterizes the quality of a predictive model by investigating the model capability to correctly predict the occurrence or non-occurrence of predefined events [52]. The AUC values vary from 0.5 to 1.0; the model is poor if AUC between 0.5 and 0.6; average if AUC between 0.6 and 0.7; good if AUC between 0.7 and 0.8; very good if AUC with the range 0.8–0.9; and excellent if AUC is greater than 0.9 [53]. For plotting ROC curve to the study area, the geographic locations of boreholes with high flow rates (8 l/s) (about 24 boreholes) were selected from the available 99 recorded boreholes. The flow rate was selected after asking many experts in the hydrogeology of the study area. The ROC for the study area is shown in Fig. 9. The AUC is 0.74 which corresponding with a prediction accuracy of 74%. Thus, the model has a good capability for producing groundwater potential zones.

6 Conclusions

A novel approach by integrating information entropy theory and weighted linear aggregation has been proposed for spatial zoning of groundwater potentiality at Altun Kupri Basin located in the north of Iraq. Entropy theory is used to assess the importance of eleven preliminary selected factors in defining groundwater potential in the basin. The groundwater potential indices are estimated using all the ten factors. The weights of the factors are assigned using entropy information theory and the ratings of the classes of each factor are assigned by AHP multi-criteria decision making. The highest entropy weights are obtained for the hydraulic head (0.233), hydraulic conductivity (0.136), elevation (0.172), and TWI (0.136). The entropy weights for other factors are found to be less than 0.1, which indicate that they are less contribution in groundwater potentiality in the basin. The results confirm the higher influence of aquifer characteristic that often excluded in study of aquifer potentiality on the spatial distribution of groundwater availability zones. Result also indicated that entropy method can be used to select the important factors responsible for groundwater occurrence of an area for rapid estimation of groundwater potential with the optimum amount of information. The method proposed in this study offers an unbiased way of assigning weights for estimation of groundwater potential reliably. Groundwater potential map of Altun Kupri Basin derived in this study could be used in exploration programs with minimum efforts. The map can also be used for sustainable management of groundwater resources in a cost-effective way.

References

1. Siebert, S.; Burke, J.; Faures, J.M.; Frenken, K.; Hoogeveen, J.; Doll, P.; Portmann, F.T.: Groundwater use for irrigation—a global inventory. Hydrol. Earth Syst. Sci. **14**, 1863–1880 (2010). doi:10.5194/hess-14-1863-2010
2. Hetzel, F.; Vaessen, V.; Himmelsbach, T.; Struckmeier, W.; Villholth, K.G.: Groundwater and Climate Change: Challenges and Possibilities. Bundesanstalt für Geowissenschaften und Rohstoffe (BGR), Hanover (2008)
3. Clifton, C.; Evans, R.; Hayes, S.; Hirji, R.; Puz, G.; Pizarro, C.: Water and climate change: impacts on groundwater resources and adaptation options. In: Water Working Notes. Note No. 25, June 2010. The Water Sector Board of the Sustainable Development Network, The World Bank Group (2010)
4. Shahid, S.; Wang, X.-J.; Keramat, M.; Akhter, G.; Farooq, S.H.; Lubis, R.F.: Vulnerability and adaptation to climate change in groundwater-dependent irrigation systems in Asian countries. APN Sci. Bull. **2014**(4), 124–126 (2014)
5. Shahid, S.; Hazarika, M.K.: Groundwater droughts in the northwestern districts of Bangladesh. Water Resour. Manage **24**(10), 1989–2006 (2010). doi:10.1007/s11269-009-9534-y
6. Alcamo, J.; Flörke, M.; Märker, M.: Future long-term changes in global water resource driven by soci-economic and climatic changes. Hydrol. Sci. J. **52**(2), 247–275 (2007). doi:10.1623/hysj.52.2.247
7. Al-Abadi, A.M.; Al-Shamma'a, A.: Groundwater potential mapping of the major aquifer in northeastern Missan Governorate, south of Iraq by using analytical hierarchy process and GIS. J. Environ. Earth Sci. **10**, 125–149 (2014)
8. Lillesand, T.M.; Kiefer, R.W.: Remote Sensing and Image Interpretation, 4th edn. Wiley, New York (2000). 804p
9. Ozdemir, A.: GIS-based groundwater spring potential mapping in the Sultan Mountains (Konya, Turkey) using frequency ratio, weights of evidence and logistic regression methods and their comparison. J. Hydrol. **411**, 290–308 (2011)
10. Al-Abadi, A.M.: Modeling of groundwater productivity in northeastern Wasit Governorate, Iraq by using frequency ratio and Shannon's entropy models. Appl. Water. Sci. (2015). doi:10.1007/s13201-015-0283-1

11. Corsini, A.; Cervi, F.; Ronchetti, F.: Weight of evidence and artificial neural networks for potential groundwater mapping: an application to the Mt. Modino area (Northern Apennines, Italy). Geomorphology **111**, 79–87 (2009). doi:10.1016/j.geomorph.2008.03.015
12. Lee, S.; Kim, Y.S.; Oh, H.J.: Application of a weight-of-evidence method and GIS to regional groundwater productivity potential mapping. J. Environ. Manage. **96**, 91–105 (2012). doi:10.1016/j.jenvman2011.09.016
13. Al-Abadi, A.M.: Groundwater potential mapping at northeastern Wasit and Missan governorates, Iraq using a data-driven weights of evidence technique in framework of GIS. Environ. Earth Sci. **74**(2), 1109–1124 (2015a). doi:10.1007/s12665-015-4097-0
14. Lee, S.; Song, K.-Y.; Kim, Y.; Park, I.: Regional groundwater productivity potential mapping using a geographic information system (GIS) based artificial neural network model. Hydrogeol. J. **20**(8), 1511–1527 (2012). doi:10.1007/s10040-012-0894-7
15. Nampak, H.; Pradhan, B.; Manap, M.A.: Application of GIS based data driven evidential belief function model to predict groundwater potential zonation. J. Hydrol. **513**, 283–300 (2014). doi:10.1016/j.jhydrol.2014.02.053
16. Mogaji, K.A.; Lim, H.S.; Abdullah, K.: Regional prediction of groundwater potential mapping in a multifaceted geology terrain using GIS-based Dempter–Shafer model. Arab. J. Geosci. **8**(5), 3235–3258 (2015). doi:10.1007/s12517-014-1391-1
17. Al-Abadi, A.M.; Pradhan, B.; Shahid, S.: Prediction of groundwater flowing well zone at An-Najif Province, central Iraq using evidential belief functions model and GIS. Environ. Monit. Assess. **188**, 549 (2016). doi:10.1007/s10661-016-5564-0
18. Rahmati, O.; Pourghasemi, H.R.; Melesse, A.M.: Application of GIS-based data driven random forest and maximum entropy models for groundwater potential mapping: a case study at Mehran Region, Iran. Catena **137**, 360–372 (2016). doi:10.1016/j.catena.2015.10.010
19. Al-Abadi, A.M.; Shahid, S.: Spatial mapping of artesian zone at Iraqi southern desert using a GIS-based random forest machine learning model. Model. Earth Syst. Environ. (2016). doi:10.1007/s40808-016-0150-6
20. Al-Abadi, A.M.; Shahid, S.; Ali, K.A.: A GIS based integration of catastrophe theory and analytical hierarchy process for mapping flood susceptibility: a case study of Teeb area. Southern Iraq. Envrion. Earth Sci. **75**, 687 (2016). doi:10.1007/s12665-016-5523-7
21. Al-Qurnawi, W.S.: Groundwater Vulnerability Assessment and Wellhead Protection Zones of Alton Kopry Basin, Kirkuk Governorate Northeast of Iraq. Unpublished Doctoral Thesis, Basra University, Iraq (2013)
22. Al Sayab, A.A.; Hassan, H.A.; Ayob, M.S.; Taha, S.H.; Salih, A.Y.; Faizi, K.N.: Water-Salt Balance and Supplementary Irrigation of Alton Copry Basin, Tech Rep. No. 14811 SRC (1983)
23. Haddad, H.R.; Al-Jawad, S.B.; Haddad, I.; Younan, A.I.; Salvo, A.V.: Hydrogeological Investigation in Jolak Basin of the Alton Copry Area. Tech. rep. no. 25. Institute for Applied Research on Natural Resources (1971)
24. Buday, T.; Jassim, S.Z.: The Regional Geology of Iraq, vol. 2: Tectonism, Magmatism, and Metamorphism. Publication of GEOSURV, Baghdad (1987)
25. Al-Naqib, K.M.: Geology of the Southern Area of Kirkuk liwa, Technical Publication. Iraq Petroleum Company Limited (1959)
26. Parson, R.M.: Groundwater Resource of Iraq, Vol. 4 Kirkuk liwa. Development Board, Ministry of Development, Government of Iraq, Baghdad (1955)
27. Al-Sudani, H.A.: Hydrogeological and Hydrochemical Properties for Groundwater System at Jolack Wadi Basin. Master Thesis, Baghdad University (1998)
28. Al-Aney, J.M.: Applied the Electrical Resistivity Method for Hydrogeologic Studies in Julak River Basin. Master Thesis, Baghdad University (1983)
29. Ozdemir, A.: Using a binary logistic regression method and GIS for evaluating and mapping the gorundwarer spring potential in the Sultan Mountians (Aksehir, Turkey). J. Hydrol. **405**, 123–136 (2011). doi:10.1016/j.jhydrol.2011.05.015
30. Oh, H.J.; Kim, Y.S.; Choi, J.K.; Park, E.; Lee, S.: GIS mapping of regional probabilistic groundwater potential in the area of Pohang City, Korea. J. Hydrol. **399**, 158–172 (2011)
31. Manap, M.A.; Sulaiman, W.N.; Ramli, M.F.; Pradhan, B.; Surip, N.: A knowledge-driven GIS modeling technique for groundwater potential mapping at the Upper Langat Basin, Malaysia. Arab. J. Geosci. **6**, 1621–1637 (2011). doi:10.1007/s12517-011-0469-2
32. Pourtaghi, Z.S.; Pourghasemi, H.R.: GIS-based groundwater spring potential assessment and mapping in the Birjand Township, southern Khorasan Province, Iran. Hydrogeol. J. **22**, 643–662 (2014). doi:10.1007/s10040-013-1089-6
33. Naghibi, S.A.; Pourghasemi, H.R.; Pourtaghi, Z.S.; Rezaei, A.: Groundwater qanat potential mapping using frequency ratio and Shannon's entropy models in the Moghan watershed, Iraq. Earth Sci. Inform. (2014). doi:10.1007/s12145-014-0145-7
34. Jenks, G.F.: The data model concept in statistical mapping. Int. Yearb. Cartogr. **7**, 186–190 (1967)
35. Moore, I.D.; Grayson, R.B.; Ladson, A.R.: Digital terrain modeling: a review of hydrological, geomorphological, and biological applications. Hydrol. Process. **5**, 3–30 (1991)
36. ESRI: Using ArcGIS Geostatistical Analyst, USA (2001)
37. Delhomme, J.P.: Kriging in the hydrosciences. Adv. Water Resour. **1**(5), 251–266 (1978)
38. Al-Abadi, A.M.; Al-Aboodi, A.D.: Optimum rain-gauges network design of some cities in Iraq. J Babylon Univ. **22**(4), 946–958 (2014)
39. Wackernagel, H.: Multivariate Geostatistics: An Introduction with Applications, 3rd edn. Springer, Berlin (2003)
40. Todd, D.K.; Mays, L.W.: Groundwater Hydrology. Wiley, New York (2005). 652p
41. WHO: Guidelines for Drinking-Water Quality, vol. 1, 3rd edn. WHO Press, Switzerland (2006)
42. Drobne, S.; Lisec, A.: Multi-attribute decision analysis in GIS: weighted linear combination and ordered weighted averaging. Informatica **33**, 459–474 (2009)
43. Eastman, R.J.: IDIRISI Andes Guide to GIS and Image Processing. Clark University, Worcester (2001)
44. Yufeng, S.; Fengxiang, J.: Landslide stability analysis based on generalized information entropy. Int. Conf. Environ. Sci. Inf. Appl. Technol. **2**, 83–85 (2009)
45. Zhi-hong, Z.; Yi, Y.; Jing-nan, S.: Entropy method for determination of weight of evaluating indicators in fuzzy evaluation for water quality assessment. J. Environ. Sci. **18**(5), 1020–1023 (2006)
46. Qiu, W.H.: Management Decisions and Entropy. Mechanical Industry Press, Beijing (2002)
47. Pei-Yue, L.; Hui, Q.; Jian-Hua, W.U.: Groundwater quality assessment based on improved quality index in Pengyang County, Ningxia, northeast China. J. Chem. **7**, 209–216 (2010)
48. Amiri, V.; Resaei, M.; Sohrabi, N.: Groundwater quality assessment using entropy weighted water quality index (EWQI) in Lenjanat, Iran. Envrion. Earth Sci. **72**(9), 3479–3490 (2014). doi:10.1007/s12665-014-3255-0
49. Yalcin, A.; Reis, S.; Aydinoglu, A.C.; Yomralioglu, T.: A GIS-based comparative study of frequency ratio, analytical hierarchy process, bivariate statistics and logistics regression methods for landslide susceptibility mapping in Trabzon, NE Turkey. Catena **85**, 274–287 (2011)
50. Saaty, T.L.: The Analytic Hierarchy Process. McGraw-Hill, New York (1980)

51. Swets, J.A.: Measuring the accuracy of diagnostic systems. Science **240**, 1285–1293 (1988)
52. Devkota, K.C.; Regmi, A.D.; Pourghasemi, H.R.; Yoshid, K.; Pradhan, B.; Ryu, I.; Dhital, M.R.; Althuwanee, O.F.: Landslide susceptibility mapping using certainty factor, index of entropy and logistic regression models in GIS and their comparison at Mugling-Narayanghat road section in Nepal Himalaya. Nat Hazards **65**, 135–165 (2013)
53. Yesilnacar, E.K.: The Application of Computational Intelligence to Landslide Susceptibility Mapping in Turkey. Ph.D. Thesis. Department of Geomatics, the University of Melbourne, pp. 423 (2005)

Arabian Journal for Science & Engineering (Springer Science & Business Media B.V.) is a copyright of Springer, 2017. All Rights Reserved.